Chemical and magnetic ordering derived from *ab initio* simulations: the case of β'-$LiFeO_2$

2010 J. Phys.: Condens. Matter 22 146008

(http://iopscience.iop.org/0953-8984/22/14/146008)

J. Phys.: Condens. Matter **22** (2010) 146008 (8pp) doi:10.1088/0953-8984/22/14/146008

Chemical and magnetic ordering derived from *ab initio* simulations: the case of β'-$LiFeO_2$

A Meyer[1], **M Catti**[2,3] **and R Dovesi**[1]

[1] Dipartimento di Chimica IFM, Università di Torino, Via Pietro Giuria 7, 10125 Torino, Italy
[2] Dipartimento di Scienza dei Materiali, Università di Milano Bicocca, Via Cozzi 53, 20125 Milano, Italy

E-mail: catti@mater.unimib.it

Received 28 January 2010, in final form 5 March 2010
Published 25 March 2010
Online at stacks.iop.org/JPhysCM/22/146008

Abstract

First-principles periodic calculations (with the B3LYP (Becke, three-parameter, Lee–Yang–Parr) hybrid functional, all-electron localized basis functions, and the CRYSTAL code) were coupled to a cluster expansion scheme in order to investigate the monoclinic β' phase of $LiFeO_2$, where a partially disordered Fe–Li distribution is observed within a rocksalt-type superstructure. By least-energy optimizing a limited number of ordered configurations, and employing a two-body truncated cluster expansion, the values $J_1 = -0.06(2)$ and $J_2 = -0.125(8)$ eV were obtained for the excess interaction energies $J_i = J_{\mathrm{LiFe},i} - (J_{\mathrm{LiLi},i} + J_{\mathrm{FeFe},i})/2$ corresponding to the first and second coordination spheres, respectively; negligible values were computed for third and further coordinations. The ordering phase transformation $\alpha \rightarrow \beta' \rightarrow \gamma$ was then addressed. Antiferromagnetic versus ferromagnetic ordering was taken into account too, and proved to lower the energy by -0.0577 eV/f.u. The corresponding cluster expansion coefficients $J_i = J_{\mathrm{AFM},i} - J_{\mathrm{FM},i}$ are $J_1 = 0.007(2)$ and $J_2 = -0.044(5)$ eV.

1. Introduction

In the search for cheaper and less toxic cathodes of lithium batteries with respect to $LiCoO_2$, the related $LiFeO_2$ compound was given considerable attention [1, 2]. This material displays many crystalline modifications stable or metastable at room temperature [3–8]. In particular, a group of them is formed by the high-temperature rocksalt-type α phase, and by its monoclinic or tetragonal β' and γ superstructures [6–8]: these were recently studied by neutron diffraction [9], finding a rather complex interplay of order–disorder and superstructure transformations on cooling. Indeed a complete disorder (α), partial disorder (β'), and full order (γ) of the Li–Fe distribution in the octahedral sites of the basic rocksalt-type structure is observed. However, the intermediate β' but not the full ordered γ phase can be synthesized at room temperature; the latter one is obtained only by annealing the β' modification. This would indicate that β'-$LiFeO_2$ is not a thermodynamically stable phase, but a frozen intermediate stage of the ordering process transforming the α into the γ polymorph. Therefore, a detailed study of the Li–Fe order–disorder state in β'-$LiFeO_2$ by computational techniques seemed to be helpful to throw light onto the peculiar behaviour of these systems. Further, owing to the magnetic properties of the Fe^{3+} ions, the aspects of ferromagnetic/antiferromagnetic ordering have to be taken into account and included in the simulations.

Theoretical investigations of the order–disorder phenomena are characterized by two features: (i) the Hamiltonian used to compute the energy of a limited number of specific ordered (fully relaxed) atomic configurations, and (ii) the heuristic model employed to interpolate/extrapolate the previous results, in order to obtain energies of a much larger number of configurations quite cheaply. As for the first point, both inexpensive semiempirical interatomic potentials and demanding *ab initio* quantum-mechanical schemes have been applied. In the present work, the latter approach will be followed, using the periodic CRYSTAL code [10] with all-electron localized atomic basis sets and a hybrid B3LYP functional. Concerning

[3] Author to whom any correspondence should be addressed.

point (ii), the cluster expansion (CE) technique [11] is the most widely utilized model: the configurational energy is expanded as a linear combination of multi-body ('clusters') atomic interaction terms of increasing complexity, with coefficients depending on the actual populations of the clusters in the configuration. Then the cluster interaction terms are best-fitted to reproduce the 'exact' energies obtained at point (i), according to a procedure also known as Connolly–Williams inversion scheme [12, 13]. This approach has been extensively applied to metal alloys [14], and occasionally to adsorbed systems [15] and to silicates [16]. Here the method is applied to an oxide system in its simplest form, where the CE is limited to two-body atomic interactions, as it was implemented and included (with the related symmetry analysis) in a new development version of the CRYSTAL code.

In summary, after briefly illustrating the computational technique used, preliminary calculations on selected ordered configurations which best represent the experimental results will be presented. Then the CE method will be applied to the chemical Li–Fe ordering, and finally to the antiferromagnetic ordering in the β'-$LiFeO_2$ crystal structure.

2. Computational

Ab initio computations of the ground-state total crystal energy were performed by use of a periodic LCAO (linear combination of atomic orbitals) approach, as implemented in the development version of CRYSTAL06 [10]. All-electron localized basis sets of Gaussian-type functions were used for the radial parts of the AO's of Fe, O and Li, corresponding to the schemes 8(s)64111(sp)411(d)G, 8(s)411(sp)1(d)G, and 5(s)11(sp)1(d)G, respectively [17]. The exponents of the outer sp Gaussians were reoptimized by energy minimization with the experimental structural parameters of $LiFeO_2$. A hybrid B3LYP functional, i.e. a balanced mixture of the DFT (density-functional-theory)-LYP non-local correlation [18] with the DFT-GGA Becke's [19] and the Hartree–Fock exchange, was employed. Owing to the $3d^5$ high-spin configuration of Fe^{3+} ions, the spin-polarized versions of the Kohn–Sham/Hartree–Fock equations were solved, yielding separate eigenvalues and eigenfunctions for the α (spin-up) and β (spin-down) electrons.

The reciprocal space was sampled according to a regular sublattice defined by a shrinking factor of four in the Monkhorst grid, so as to give rise to 24 independent points in the irreducible Brillouin zone (monoclinic case). The five tolerances related to cut-off limits for series summation were set to 10^{-7}, 10^{-7}, 10^{-7}, 10^{-7}, and 10^{-14}. Convergence was also controlled by a ΔE threshold of 10^{-7} Hartree per primitive unit-cell in the SCF cycles. The integration of the DFT functionals was performed by use of the XLGRID accuracy conditions [10]. In order to accelerate the SCF convergence, the technique of level shifter was used [20, 21], enhancing the energy difference between highest occupied and lowest empty states in the first cycles. Atomic coordinates were optimized by calculation of analytical gradients and subsequent conjugate gradients algorithm (OPTCOORD option [10]).

3. Least-energy Li–Fe ordered structure of β'-$LiFeO_2$

Two ordered structural models (monoclinic $C2/c$ and tetragonal $I4_1/amd$) were originally proposed for the β' polymorph of $LiFeO_2$, corresponding substantially to different representations of the same superstructure of the disordered rocksalt-type α phase [22]. In both cases, O atoms are in the ideal FCC arrangement and four independent cation sites in the octahedral holes are occupied by two Fe and two Li atoms. However, the $C2/c$ conventional unit-cell contains eight formula units ($Z = 8$), whereas $Z = 32$ for the tetragonal case.

On the basis of a recent neutron powder diffraction study of this phase [9], its crystal structure was Rietveld-refined satisfactorily according to a partially disordered version of the $C2/c$ model (agreement index $wR_p = 7.1\%$). The $I4_1/amd$ model could also be refined, but it gave significantly worse results ($wR_p = 12.1\%$). In both cases, two of the four cation sites were pure Fe and Li, respectively, and the other two were Fe–Li statistical mixtures with 0.56(2) and 0.44(2) refined occupation fractions. This partial disorder was ascribed to the β' phase being an intermediate stage of the Fe/Li ordering process from the (fully disordered) α to the (fully ordered) γ modification.

In order to understand the physical origin of the phenomenon, the different possible ordered configurations of the β' crystal structure have to be considered and ranged according to their energies. Let us call s1, s2, s3, and s4 the four cation sites (4e Wyckoff positions $0, y, 1/4$ of the $C2/c$ space group) with ideal y values of $1/16$, $5/16$, $9/16$, $13/16$, respectively. According to the experimental results, s1 and s3 are Fe–Li mixtures, s2 is pure Fe and s4 is pure Li [9]. The six possible ordered distributions of two Fe and two Li atoms over the four sites can be divided in two groups: four with neighbouring Fe–Fe and Li–Li pairs (alike atoms are separated by $\Delta y = 1/4$), and two with alternating Fe–Li–Fe–Li atoms along the [010] twofold axis ($\Delta y = 1/2$). Let us call them configurations A and B, respectively. Both ordering schemes consistent with the experimental structure, i.e. s1(Fe)s2(Fe)s3(Li)s4(Li) and s1(Li)s2(Fe)s3(Fe)s4(Li), belong to configuration A (figure 1). Their expected statistical weight in the average structure should be close to 0.5, according to the refined Fe and Li occupation factors on the s1 and s3 sites. An example of configuration B is s1(Fe)s2(Li)s3(Fe)s4(Li).

The ground-state total energy was computed for configurations A and B, relaxing the monoclinic lattice constants and the ten atomic fractional coordinates unconstrained by the $C2/c$ symmetry. A ferromagnetic state was assumed with electron spin-up on all Fe atoms in the unit-cell. The starting geometries were the ideal ones, corresponding to the atomic coordinates of the FCC arrangement. All configurations corresponding to model A proved to be degenerate in energy, and the same was for those of model B. In table 1, the results are reported and compared to the outcome of the neutron diffraction study. Model A is clearly favoured over B, with an energy gain of -1.70 mHartree/f.u. (-0.046 eV/f.u.). Further, the optimized

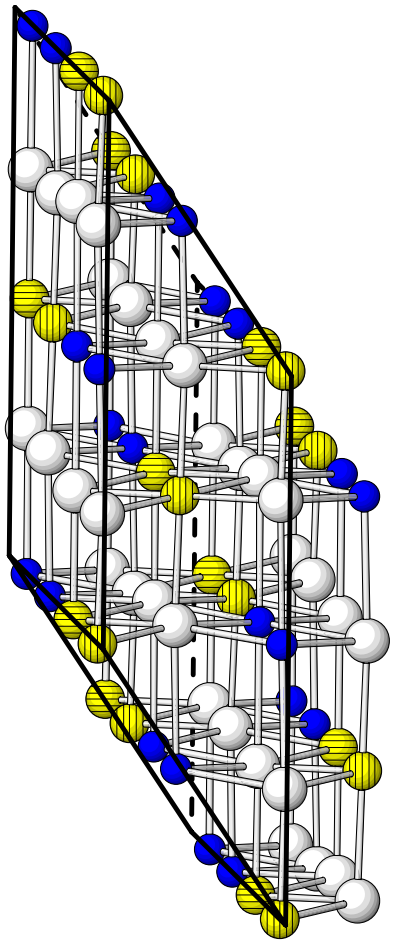

Figure 1. Ordered $C2/c$-A structure of monoclinic β'-$LiFeO_2$, viewed along [010]. The least-energy antiferromagnetic spin arrangement is shown. Spheres with horizontal and vertical hachure denote spin-up (α) and spin-down (β) polarized Fe atoms. Dark (blue) and white spheres indicate Li and O atoms, respectively. (This figure is in colour only in the electronic version)

Table 1. Least-energy optimized configurations of the $C2/c$-A and $C2/c$-B ordered models of the crystal structure of β'-$LiFeO_2$, compared to neutron diffraction results [9]. A ferromagnetic spin arrangement is assumed for Fe atoms.

	$C2/c$-A	$C2/c$-B	Experimental
a (Å)	8.662	8.200	8.566
b (Å)	11.704	12.252	11.574
c (Å)	5.259	5.066	5.197
β (deg)	146.16	144.02	146.06
y (s1)	0.0586 (Fe)	0.0732 (Fe)	0.063 (Fe–Li)
y (s2)	0.3156 (Fe)	0.3010 (Li)	0.313 (Fe)
y (s3)	0.5672 (Li)	0.5732 (Fe)	0.562 (Li–Fe)
y (s4)	0.8079 (Li)	0.8010 (Li)	0.850 (Li)
x (O1)	0.2370	0.2500	0.244
y (O1)	0.0621	0.0504	0.064
z (O1)	0.2513	0.2501	0.265
x (O2)	0.2466	0.2500	0.249
y (O2)	0.3127	0.3204	0.312
z (O2)	0.2692	0.2500	0.267
E (Hartree/f.u.)	−1421.796 597	−1421.794 895	

Table 2. Metal–oxygen bond distances (Å) in the optimized configurations of the ordered models $C2/c$-A and $C2/c$-B of the crystal structure of β'-$LiFeO_2$, compared to neutron diffraction results [9].

	$C2/c$-A	$C2/c$-B	Experimental
Fe(s1)–O	2.042 × 2	1.979 × 2	2.02 × 2
	2.048 × 2	2.069 × 2	2.03 × 2
	2.064 × 2	2.124 × 2	2.10 × 2
Average	2.051	2.057	2.05
Fe(s2)–O	2.048 × 2	1.979 × 2	2.00 × 2
	2.053 × 2	2.069 × 2	2.02 × 2
	2.061 × 2	2.123 × 2	2.06 × 2
Average	2.054	2.057	2.03
Li(s3)–O	2.075 × 2	2.064 × 2	2.03 × 2
	2.105 × 2	2.104 × 2	2.09 × 2
	2.285 × 2	2.351 × 2	2.26 × 2
Average	2.155	2.173	2.13
Li(s4)–O	2.079 × 2	2.064 × 2	1.80 × 2
	2.119 × 2	2.102 × 2	2.27 × 2
	2.281 × 2	2.353 × 2	2.41 × 2
Average	2.160	2.173	2.16

lattice constants and atomic coordinates of model A are in good agreement with the corresponding experimental values, whereas strong deviations are observed between the latter ones and results of model B. The only significant difference of the optimized model A with respect to the refined structure concerns the y coordinate of Li in s4. This Li atom is displaced from the centre ($y = 0.8125$) of its coordination octahedron in the experimental structure, but such a feature is not appreciably present in the computed configuration. In table 2, the Fe–O and Li–O interatomic distances are reported for both ordered models and for the average experimental structure. Again, the values for configuration A agree very well with experimental results, except for the Li(s4)–O distances. We conclude that the distortion observed in the refined structure, but not in the theoretical local model, should be related somehow to the averaging due to disorder.

The fact that the experimentally observed average structure of β'-$LiFeO_2$ is compatible with ordering schemes of type A but not B is explained by the second configuration being less stable than the first one. A simple justification of this result can be found by considering the repulsive electrostatic interaction of Fe^{3+} and Li^+ ions with those belonging to the first cation–cation coordination sphere (C.N. = 12, radius about 3 Å). In configuration A, each of the two Fe^{3+} ions is surrounded by seven Li^+ and five Fe^{3+} ions (and each Li^+ is surrounded by five Li^+ and seven Fe^{3+}), whereas in case B each cation has six Li^+ and six Fe^{3+} ions as first neighbours. By summing the products of ionic charges, one obtains $5(q_{Fe}^2 + q_{Li}^2) + 7q_{Fe}q_{Li}$ in case A, and $6(q_{Fe}^2 + q_{Li}^2) + 6q_{Fe}q_{Li}$ in case B. The difference is negative, so that the electrostatic cation–cation repulsion is smaller in the A than in the B configuration. The result is not changed by including the second coordination sphere (C.N. = 6, radius about 4 Å), as in both cases there are two unlike and four alike ions on the sphere, with respect to the central ion. The list of cation–cation distances for models A and B is reported in table 3. Though very crude, a simple electrostatic model is thus able to explain qualitatively some

Table 3. Metal–metal interatomic distances (Å) in the optimized configurations of the ordered Models $C2/c$-A and $C2/c$-B of the crystal structure of β'-$LiFeO_2$.

	$C2/c$-A	$C2/c$-B
Fe(s1)	Li 2.931 × 2	Li 2.792
	Li 2.935	Li 2.965 × 2
	Fe 2.966 × 2	Li 2.966 × 2
	Fe 2.987 × 2	Fe 2.977 × 2
	Li 2.987 × 2	Fe 3.103 × 2
	Fe 3.008	Fe 3.104 × 2
	Li 3.058 × 2	Li 3.336
	Fe 4.083 × 2	Li 4.079 × 2
	Li 4.134 × 2	Fe 4.100 × 2
	Li 4.332 × 2	Li 4.470 × 2
Fe(s2)	Li 2.931 × 2	Li 2.790
	Li 2.944	Li 2.965 × 2
	Li 2.966 × 2	Li 2.967 × 2
	Fe 2.987 × 2	Fe 2.977 × 2
	Li 3.001 × 2	Fe 3.103 × 2
	Fe 3.008	Fe 3.103 × 2
	Fe 3.019 × 2	Li 3.334
	Fe 4.083 × 2	Li 4.081 × 2
	Li 4.128 × 2	Fe 4.100 × 2
	Li 4.332 × 2	Li 4.471 × 2

of the Li/Fe ordering features, even by consideration of real reduced atomic charges with respect to ideal ionicity (table 4).

In order to study possible ordered schemes with a lower symmetry than the $C2/c$ space group, its $C2$ subgroup was selected, as (unlike Cc or $C\bar{1}$) it produces a doubling of the number of independent cation sites. First of all, the A and B configurations of the first four sites at $0, y, 1/4$ can be associated to the corresponding occupation patterns A′ (Fe′–Fe′–Li′–Li′) and B′ (Fe′–Li′–Fe′–Li′) of the other four sites (s1′, s2′, s3′, s4′) at $0, y, 3/4$. The $C2$-AA′ and $C2$-BB′ configurations are obviously equivalent to $C2/c$-A and $C2/c$-B, respectively. On the other hand, the $C2$-AB′ (or $C2$-BA′) configuration is new: half cations have an environment of seven unlike and five like ions, and the other half are surrounded by six unlike and six alike cations. The computed energy of the relaxed $C2$-AB′ structure is −1421.795 129 Hartree/f.u., and then only slightly lower than that of model $C2/c$-B. Second, two additional new structures can be generated, with Fe–Fe–Fe–Li/Li′–Li′–Li′–Fe′ ($C2$-D) and Fe–Fe–Fe–Fe/Li′–Li′–Li′–Li′ ($C2$-E) configurations. Their energies, after full structural relaxation, are −1421.790 843 and −1421.780 566 Hartree/f.u., respectively. It can thus be concluded that no energy improvement is brought about by devising ordered schemes with lower symmetry than $C2/c$.

As a last point, we also considered ordered structural models of β'-$LiFeO_2$ within the $I4_1/amd$ representation. In this case three different configurations consistent with the full symmetry are obtained: A, B, and C. The first two are exactly the same as the corresponding ones in $C2/c$ (A: seven unlike and five alike first neighbours; B: six unlike and five alike), and the energies of the optimized structures are also very similar (−1421.796 557 and −1421.794 289 Hartree, respectively). The C configuration has a higher energy (−1421.790 057 Hartree) and a less favourable coordination environment of cations (five unlike and seven alike first neighbours). In all three cases there are four unlike and two alike second neighbours. It is also confirmed that the energy increases with the number of alike cations in the first cation coordination sphere. It should be remarked that the $C2/c$-A structural model is slightly more stable (by 0.04 mHartree) than the $I4_1/amd$-A, consistent with the results of the Rietveld refinement of the experimental neutron diffraction results.

Table 4. Mulliken atomic charges and iron magnetic moments (atomic units) in $C2/c$-A β'-$LiFeO_2$.

q_{Li}	0.95
q_{Fe}	1.86
q_{O1}	−1.38
q_{O2}	−1.42
μ_{Fe} (FM)	4.21
μ_{Fe} (AFM)	4.24

4. Two-body cluster expansion model of disorder

Section 3 was focused on the search of the least-energy ordered ferromagnetic configuration for the structure of β'-$LiFeO_2$, taking into account the consistency with experimental neutron diffraction data. Here the problem is tackled from a wider point of view: can we estimate the energies of all possible ordered configurations, by interpolation/extrapolation from a limited number of accurate *ab initio* energies? This problem can be solved by the cluster expansion model [11–13], which in our case is limited to the first-order (two-body clusters) approximation. The ordering energy of any configuration is assumed to be a function only of cation–cation interaction energies ($J_{FeFe,i}$, $J_{LiFe,i}$, $J_{LiLi,i}$) indexed on two-body distances i, multiplied by the numbers n_i of corresponding atomic pairs.

The excess energy (difference with respect to the average energy of the two pure Li and Fe end-members) depends only on the mixed $n_{LiFe,i}$ populations and on the excess interaction energies $J_i = J_{LiFe,i} - (J_{LiLi,i} + J_{FeFe,i})/2$, according to:

$$E_{exc} = (1/2) \sum_i n_{LiFe,i} J_i. \quad (1)$$

The number of unknown J_i parameters equals that of cation–cation coordination shells which are considered. At least as many (but possibly more) linear equations of type (1) have to be set up for the corresponding number of configurations. The energy values are computed quantum-mechanically with full structural relaxation, and the $n_{LiFe,i}$ coefficients define every configuration considered. Once the interaction parameters J_i have been determined by solving the equations, the formula (1) can be applied to estimate the excess energy of any ordered configuration outside the small group previously employed.

The whole procedure was implemented inside the development version of the CRYSTAL code in five steps: (i) definition of the two-body coordination spheres, with possible grouping of distances within shells of given radial thicknesses; (ii) definition of the symmetry-unrelated classes of ordered configurations, including the set of n_i population coefficients for each class and each coordination shell;

Table 5. Average first-(1) and second-(2) neighbours coordination numbers of cations, and relative energies (eV/f.u.) of the ordered models of monoclinic β'-$LiFeO_2$.

	(1)		(2)		
	Fe–Li	Fe–Fe or Li–Li	Fe–Li	Fe–Fe or Li–Li	ΔE
$C2/c$-A	7	5	4	2	0
$C2/c$-B	6	6	4	2	0.0463
$C2$-AB′	6.5	5.5	4	2	0.0399
$C2$-D	7	5	3	3	0.1566
$C2$-E	8	4	0	6	0.4362

(iii) selection of the set of configurations for the full quantum-mechanical calculation; (iv) solution by least-squares method of the corresponding set of equation (1) in the unknown J_i parameters; (v) estimate of the energies of other configurations by equation (1) and possible iterative process from (iii).

Starting from the monoclinic structure of β'-$LiFeO_2$, there are 38 symmetry-unrelated ways of distributing four Fe and four Li atoms over the eight sites available in the primitive unit-cell. Six configurations keep the $C2/c$ symmetry, but only two of them, $C2/c$-A and $C2/c$-B, are really independent (cf section 3). Thirty-two configurations belong to the $C2$ space group, generating three independent ones: $C2$-AB′, $C2$-D and $C2$-E. Thus, only the set of five ordered structures outlined in section 3 need to be considered.

In table 5, the coordination numbers of a single cation site for unlike (Fe–Li) and alike (Fe–Fe or Li–Li) metal neighbours, in the first and second coordination spheres, are reported for all five configurations. In the $C2$-AB′ case, first sphere, a metal site has seven unlike and five alike neighbours, and another one has six and six, so that the corresponding average values are given. The coefficients $n_{\mathrm{LiFe},i}$ appearing in equation (1) are obtained by multiplying the values of the Fe–Li columns (table 5) by eight, which is the number of cations per unit-cell. In this way the E_{exc} value of equation (1) is referred to a unit-cell.

All interactions within a 4.5 Å range can be grouped into two values: J_1 and J_2 (first and second coordination shells, respectively). The excess energies of equation (1) are obtained by subtracting the total energy of one of the configurations from those of the other ones. Then the equation of $C2/c$-A was subtracted from the other ones obtaining four equations in the two unknowns J_1 and J_2. The solution gives $J_1 = -0.06(2)$ and $J_2 = -0.125(8)$ eV, with the e.s.d.'s in parentheses. We also tried to include a further interaction energy J_3, accounting for the third coordination shell grouping distances around 5 Å: however, the value fitted for J_3 was four orders of magnitude smaller than J_1 and J_2, so as to be considered as negligible.

The negative signs of J_1 and J_2 confirm that the Fe^{3+}–Li^+ pairing in the first and second coordination shells stabilizes the configuration with respect to Fe^{3+}–Fe^{3+} and Li^+–Li^+ pairings, as argued on simple electrostatic principles in section 3. Surprisingly, the effect is larger for the second than for the first shell: this appears also clearly by inspection of table 5, where the strong increase of ΔE on decreasing the number of Fe–Li second neighbours looks remarkable. In order to check the previous results, the problem was tackled with reference to the tetragonal $I4_1/amd$ structural model of $LiFeO_2$ [9, 22]. In this case the unit-cell contains four times the number of atoms of the monoclinic one, and then many more configurations (70 instead of 38) are accessible, although the point-group symmetry is higher. Six ordered configurations keeping the $I4_1/amd$ symmetry were selected. The J_1 and J_2 values obtained by solving five linear equations were $-0.084(5)$ and $-0.131(3)$ eV, respectively. The J_2 interaction energy is close to the previous value; $|J_1|$ is somehow larger than the monoclinic result, but it is confirmed to be substantially smaller than $|J_2|$.

In order to understand the relative magnitudes of J_1 and J_2, the effect of structure relaxation was examined. The energies of the five configurations were recalculated with fixed geometries (ideal atomic coordinates derived from the rocksalt structure), and the J_1 and J_2 parameters were fitted to them, obtaining -0.308 and -0.231 eV, respectively (monoclinic) and -0.378 and -0.269 eV (tetragonal). The $|J_1|$ and $|J_2|$ values are obviously much larger than in the previous case, because the structures were not let to relax so as to partly compensate for the unfavourable cation arrangements. However, the important result is that the J_1/J_2 ratio changes from 0.48 to 1.33 (monoclinic) or from 0.65 to 1.40 (tetragonal) when the relaxation effect is removed. In this case, it can be noticed that $J_1/J_2 \cong r_2/r_1$, where r_1 and r_2 are the average radii of the first and second coordination shells; thus, the two energy parameters follow the Coulomb law, and $|J_1| > |J_2|$ accordingly. On the other hand, the J_1/J_2 ratio drops dramatically below one when the structure is allowed to relax, because the screening effect of relaxation is stronger at shorter distances and then affects J_1 more than J_2: $|J_1| < |J_2|$ ensues.

A study of the temperature dependence of the Li–Fe order–disorder would require full Monte Carlo (MC) simulations based on the CE energy (1), according to well established procedures [13]; this is outside the scope of the present work. One can attempt to roughly estimate the disordering temperature by simple approximations such as $T_{\mathrm{D}} \sim (\Delta E_{\mathrm{D}} - \Delta E_{\mathrm{O}})/\Delta S_{\mathrm{D}}$ from [12], where ΔS_{D} is the ideal mixing entropy. In our case the disordered (D) state refers to six and three average Fe–Li first and second coordination numbers, whereas the ordered (O) configuration corresponds to the experimental $C2/c$-A structure with seven and four values, respectively (cf table 5). By use of equation (1), one thus obtains $T_{\mathrm{D}} \sim (-J_1 - J_2)/k_{\mathrm{B}} \ln 2 = 3097$ K, which is clearly overestimated with respect to the observed β' to α phase transformation of $LiFeO_2$ at 923 K [9]. The main reason is that short-range order should be present also in the long-range disordered phase, thus reducing ΔE_{D} and then lowering T_{D}. Of course a thorough statistical sampling of the energy (1) by MC techniques would be necessary to account for the process properly.

5. Antiferromagnetic ordering

The two-body cluster expansion model can be applied also to spin ordered magnetic configurations, and in this version it is better known as Ising model. Here the excess energy

of equation (1) is the difference antiferromagnetic (AFM)–ferromagnetic (FM). The attention is focused only on Fe^{3+} ions, carrying a formal spin moment of 5 μ_B which is now not always positive as in the previous ferromagnetic case, but positive on half of the atoms in the unit-cell and negative on the other half (antiferromagnetic ordering). Each AFM configuration is defined by the distribution of up- and down-spins over the available Fe sites.

Let us start from the $C2/c$-A chemical configuration, where there are four Fe sites per unit-cell and then six AFM ordered arrangements are possible. Only three of them are independent: s1(Fe↑)s2(Fe↓)s1′(Fe↑)s2′(Fe↓), keeping the $C2/c$ symmetry, and s1(Fe↑)s2(Fe↑)s1′(Fe↓)s2′(Fe↓) and s1(Fe↑)s2(Fe↓)s1′(Fe↓)s2′(Fe↑), downgrading the symmetry to $C2$. Similarly, the $C2/c$-B configuration gives rise to the three independent AFM arrangements s1(Fe↑)s3(Fe↓)s1′(Fe↑)s3′(Fe↓) ($C2/c$), s1(Fe↑)s3(Fe↑)s1′(Fe↓)s3′(Fe↓) ($C2$) and s1(Fe↑)s3(Fe↓)s1′(Fe↓)s3′(Fe↑) ($C2$).

The energies of all these six AFM configurations were calculated, keeping the structural geometry fixed at the values optimized for the $C2/c$-A and $C2/c$-B FM cases (table 1). Indeed, changing the magnetic ordering from FM to AFM is expected to induce a very small structure relaxation (cf the results below). The most stable AFM arrangement turns out to be s1(Fe↑)s2(Fe↓)s1′(Fe↓)s2′(Fe↑) ($C2$), with $E = -1421.798\,713$ Hartree/f.u. and a gain of -0.0577 eV/f.u. with respect to the corresponding FM case (figure 1). A minor change is observed in the magnetic moment of iron, by comparison with the FM structure (table 4): in both cases, over 80% of the $3d^5$ electrons are polarized.

As for the Ising model, the first two Fe–Fe coordination spheres, corresponding to shells around radii of 3 and 4 Å respectively (table 3), define the interaction parameters J_1 (first coordination) and J_2 (second coordination). We have thus six equations of type (1) in the J_1 and J_2 unknowns (from which the equation for the FM case has to be subtracted), derived from the A and B models. By solving the least-squares linear system, the following values were obtained for the interaction energies: $J_1 = 0.007(2)$, and $J_2 = -0.044(5)$ eV, with the e.s.d.'s in parentheses. The small, positive J_1 value means that the Fe↑–O–Fe↓ AFM coupling is slightly unfavoured with respect to the Fe↑–O–Fe↑ FM one for the first coordination sphere (cf the Fe–O–Fe angles of about 90°, unfit to superexchange bond geometry). On the other hand, the strongly negative J_2 interaction is responsible for the stabilization of the AFM versus FM ordering, consistent with the superexchange-fit Fe–O–Fe bonding angle of 180° in the second coordination sphere.

We also decided to check the effect of the unit-cell size on the AFM interactions. Therefore, a supercell of the standard monoclinic cell with fourfold volume was considered, choosing the transformation matrix 010/204/100 which minimizes the cell anisotropy. There are now 16 sites, instead of four, for the Fe magnetic atoms in the primitive cell. Again, the magnetic arrangements were limited to those derived from the $C2/c$-A and $C2/c$-B chemical configurations. Two systems of 13 equations in the three unknowns J_1, J_2, and J_3 were then considered and solved. The values obtained for the first two parameters confirm substantially those coming from the smaller cell; J_3 is negligible, indicating that the third coordination interactions are not significant. An iterative search for the most stable AFM configuration showed it to be of type A, with an energy of $-1421.799\,070$ Hartree/f.u. and then with a minor gain of -0.0098 eV/f.u. with respect to the least-energy configuration of the small cell. This means that the monoclinic unit-cell of table 1 is quite adequate to produce a satisfactory AFM model structure, although the symmetry decreases from $C2/c$ to $C2$.

A test was also made to check the possible structure relaxation of the (big cell) AFM least-energy configuration. The energy was lowered by only -0.0035 eV/f.u., so that the magnetic ordering was confirmed to affect the geometric structure in a negligible way. For the sake of completeness, the AFM ordering was studied also within the frame of the tetragonal $I4_1/amd$ structural model. The size of the primitive

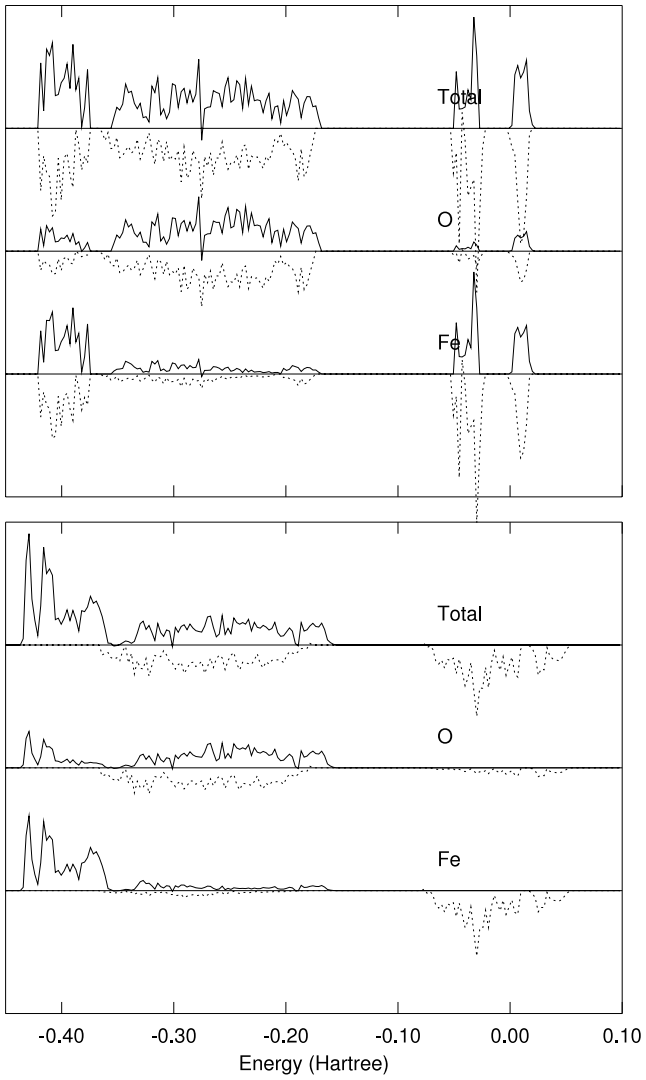

Figure 2. Total and O, Fe projected electron DOS of the FM (bottom) and AFM (top) structures of monoclinic β'-$LiFeO_2$. The top of valence band lies at -0.156 and -0.167 Hartree, respectively. Full and dashed lines refer to α and β spin states.

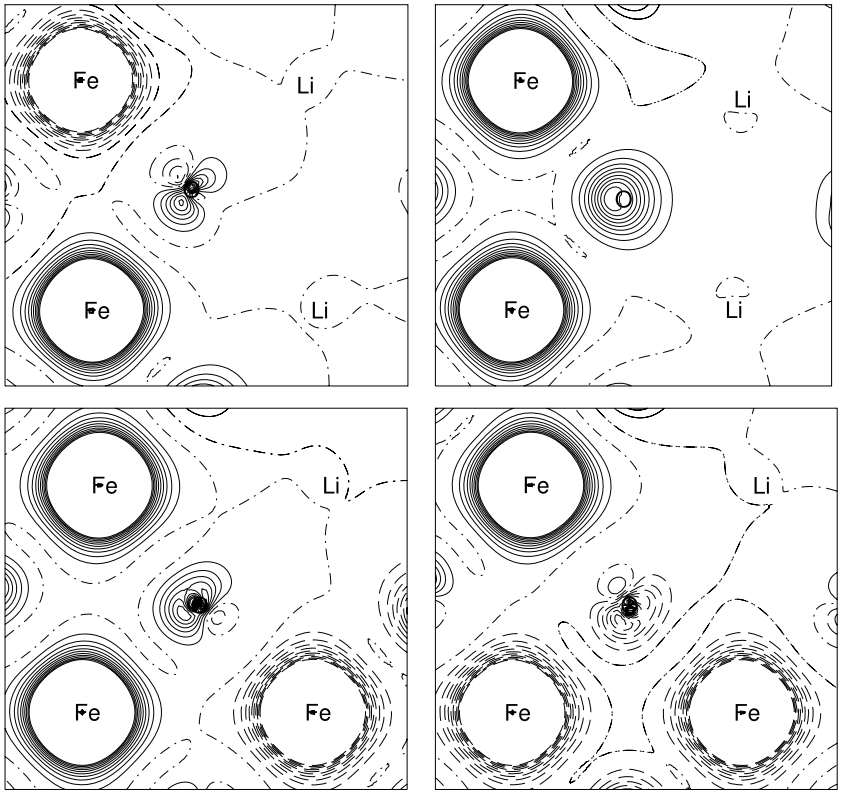

Figure 3. Spin density $\rho_\alpha - \rho_\beta$ maps centred around four O atoms in the antiferromagnetic structure of monoclinic β'-$LiFeO_2$. The contour lines are separated by 0.01 au (e bohr^{-3}). Full, dashed and dashed–dotted lines indicate positive, negative and zero values, respectively. The total spin populations of the four O atoms are (left to right, and top to bottom) 0.118, 0.359, 0.127, and 0.113 (electron units).

unit-cell is the same as that of the big monoclinic cell ($Z = 16$, 64 atoms). A quite similar scheme was followed for this analysis, obtaining consistent results for the J_1, J_2, and J_3 parameters.

The computed electron densities of states (DOS) of the FM and AFM monoclinic structures of β'-$LiFeO_2$ are shown in figure 2. The corresponding energy gaps are 2.21 (FM) and 3.16 (AFM) eV. In both cases, the valence band is formed by a lower-energy part contributed by fully spin-polarized Fe states, and by an upper-energy part due to O states with minor spin polarization. The conduction band is essentially due to spin-polarized Fe levels. The α and β Fe states in the same energy range (AFM structure) never belong to the same atom, unlike the case for O states (FM and AFM structures). It is interesting to examine the partial spin polarization of O atoms in the AFM configuration. This can be appreciated by considering maps of the electron spin density $\rho_\alpha - \rho_\beta$ around four different kinds of O atoms (figure 3). Each O atom is surrounded by a coordination octahedron formed by three Fe and three Li atoms, which is cut in the middle by the map plane. In the two upper sections of figure 3, an α-Fe and a Li atom lie above and below the plane, respectively; in the lower ones, two Li atoms do. The Mulliken α–β spin populations given in the caption of figure 3 show two kinds of O atoms: those surrounded by three Fe atoms with parallel spins have a quite large spin polarization of the same sign, amounting to more than (1/3)e; the other ones decrease their polarization more than proportionally to the number of antiparallel polarized neighbouring Fe atoms.

6. Conclusions

The Li/Fe partially disordered monoclinic structure of β'-$LiFeO_2$ was studied by quantum-mechanical simulations, so as to assess the energetic hierarchy of ordered configurations. It was shown that the cluster expansion model limited to two-body terms is a sufficient approximation to model this type of system, where chemical bonding is mostly ionic. However, the second coordination sphere gives rise to a larger interaction parameter (J_2) than the first one (J_1), unlike what would appear from simple electrostatic considerations; further coordination spheres give negligible contributions to the energy. The effect of ignoring multi-body terms in the cluster expansion is roughly measured by the estimated uncertainties of J_1 and J_2.

On cooling, the driving force of the ordering process from the α to the β' and γ phases of $LiFeO_2$ is the energy gain of maximizing the number of Fe–Li with respect to Fe–Fe and Li–Li neighbours. The residual disorder in the β' phase is due to coexistence of two energy degenerate configurations of model A, so that further ordering on cooling is difficult. Thus, annealing is necessary to overcome the kinetic barrier leading to the fully ordered structure of the γ phase.

The cluster expansion technique was also applied to study a wide range of possible antiferromagnetically ordered structures of the β' phase. Antiferromagnetic ordering was shown to bring about a significant energy gain over the ferromagnetic structure, without change of the unit-cell. Neutron diffraction studies at low temperature should be performed on β'-$LiFeO_2$ to verify this result.

Acknowledgment

The research was supported by a PRIN grant of MIUR, Rome (Cofin07 Project 200755ZKR3_004).

References

[1] Matsumura T, Kanno R, Inaba Y, Kawamoto Y and Takano M 2002 *J. Electrochem. Soc.* **149** A1509
[2] Kanno R, Shirane T, Kawamoto Y, Takeda Y, Takano M, Ohashi M and Yamaguchi Y 1996 *J. Electrochem. Soc.* **143** 2435
[3] Douakha N, Holzapfel M, Chappel E, Chouteau G, Croguennec L, Ott A and Ouladdiaf B 2002 *J. Solid State Chem.* **163** 406
[4] Tabuchi M, Ado K, Kobayashi H, Matsubara I, Kageyama H, Wakita M, Tsutsui S, Nasu S, Takeda Y, Masquelier C, Hirano A and Kanno R 1998 *J. Solid State Chem.* **141** 554
[5] Armstrong A R, Tee D W, La Mantia F, Novak P and Bruce P G 2008 *J. Am. Chem. Soc.* **130** 3554
[6] Cox D E, Shirane G, Flinn P A, Ruby S L and Takei W J 1963 *Phys. Rev.* **132** 1547
[7] Anderson J C and Schieber M 1964 *J. Phys. Chem. Solids* **25** 961
[8] Tabuchi M, Ado K, Sakaebe H, Masquelier C, Kageyama H and Nakamura O 1995 *Solid State Ion.* **79** 220
[9] Barré M and Catti M 2009 *J. Solid State Chem.* **182** 2549
[10] Dovesi R, Saunders V R, Roetti C, Orlando R, Zicovich-Wilson C, Pascale F, Civalleri B, Doll K, Harrison N M, Bush I J, D'Arco Ph and Llunell M 2006 *CRYSTAL06: User's Manual* University of Torino, Italy
[11] Sanchez J M, Ducastelle F and Gratias D 1984 *Physica* A **128** 334
[12] Connolly J W D and Williams A R 1983 *Phys. Rev.* B **27** 5169
[13] Mueller S 2003 *J. Phys.: Condens. Matter* **15** R1429
[14] Liu J Z, van de Walle A, Ghosh G and Asta M 2005 *Phys. Rev.* B **72** 144109
[15] Sluiter M H F and Kawazoe Y 2003 *Phys. Rev.* B **68** 085410
[16] Becker U and Pollok K 2002 *Phys. Chem. Miner.* **29** 52
[17] http://www.crystal.unito.it
[18] Lee C, Yang W and Parr R G 1988 *Phys. Rev.* B **37** 785
[19] Becke A D 1993 *J. Chem. Phys.* **98** 5648
[20] Saunders V R and Hillier I H 1973 *Int. J. Quantum Chem.* **7** 699
[21] Guest M F and Saunders V R 1974 *Mol. Phys.* **28** 819
[22] Brunel M and de Bergevin F 1968 *J. Phys. Chem. Solids* **29** 163